Historical change of El Niño properties shed light on future changes of extreme El Niño

Bin Wang, Xiao Luo, Young-Min Yang, Weiyi Sun, Mark A. Cane, Wenju Cai, Sang-Wook Yeh, and Jian Liu

PNAS Nov 2019

Motivation

- El Niño's intensity change under increased greenhouse warming is of great societal concern, yet climate models' projections remain largely uncertain (Yeh et al. 2009, Cai et al. 2018).
- Besides the model approach, understanding how El Niño properties have changed in the context of the 20th century's global warming may shed light on El Niño's future change.
- Special effort is to unravel the controlling factors that lead to more frequent occurrence of large-amplitude El Niño events.
- The current classification of El Niño does not distinguish the strong from moderate El Niño events, making it difficult to project future change of El Niño's intensity.

How has El Nino been classified?

Capotondi et al. (2015) Understanding El Nino Diversity, BAMS

Definitions of El Niño types often vary with the method used.

- a) El Niño Modoki index (EMI) method (Ashok et al. 2007):
- B) Niño-3–4 index (Kug et al. 2009; Yeh et al. 2009): “warm pool” , “Cold tongue”
- c) EP–CP index method (Kao and Yu 2009; Yu et al. 2012):
- d) E and C indices (Takahashi et al. 2011):
- e) EP–CP subsurface index method (Yu et al. 2011):
- f) Sea surface salinity (SSS) index method (Singh et al. 2011; Qu and Yu 2014):
- g) Outgoing longwave radiation (OLR) index method (Chiodi and Harrison 2013):

Timmermann et al. (2018) ENSO complexity, Nature

When El Niño events are viewed as superposition of the two leading EOF modes of tropical Pacific SST anomalies, results in a continuum of ENSO characteristics that capture a mix of EP and CP dynamics (e.g. 1991/92 and 2015/16 events) (Giese & Ray, 2011; Johnson, 2013).

Problems with the current classification of El Nino

- The identified CP and EP El Niño events vary considerably among different authors The commonly recognized years of CP El Niño events are 1994, 2002, 2004, 2009; other disputed years include 1986, 1987, 1990, 1991, 1992, and 2006 (Capotondi et al., 2015; Xiang et al., 2013).
- Use of different variable and methods,
- Subjective criteria,
- Insufficient samples.
- The inconsistency in the identified CP and EP El Niño events and failure to distinguish strong from moderate events impedes investigation of their respective dynamics, predictability, climate impacts, and changes in the past and future.

How to better delineate El Nino diversity?
Recipes

- Focus on temporal-spatial structure from pre-onset to development processes rather than just spatial structure at mature phase.
- Use Objective methods
- Use as long as possible historical records.
- On a firm physical basis—coupled dynamical processes

Data

SST : Merged datasets from

(1) 1870-2017 HadISST (HadISST 1.1 monthly average SST);

(2) NCEP OI SST(NOAA Extended Reconstructed SST V5)..

Ocean reanalysis datasets

(1) SODA version 2.2.4 reanalysis for 1871-2008;

(2) Global Ocean Data Assimilation System (GODAS) from 2009 to 2018.

Atmospheric reanalysis

(1) The merged NCEP dataset: NOAA-CIRES Twentieth Century Reanalysis (20CRv2c) (1871-2012) and NCEP/DOE Reanalysis 2 data (1979-2018);

(2) The merged ECMWF reanalysis dataset: ERA-20C reanalysis (1901 to 2010), the ERA 40-year (ERA-40) reanalysis (1958 to 2001) and the ERA-Interim reanalysis (1979 to 2018).

The land precipitation data:

(1) Global Precipitation Climatology Center (GPCC) dataset over land 1901 - 2017

(2) Climate Research Unit (CRU) TS v. 4.02 land precipitation 1901-2017.

Definition of El Niño years (1901-2017)

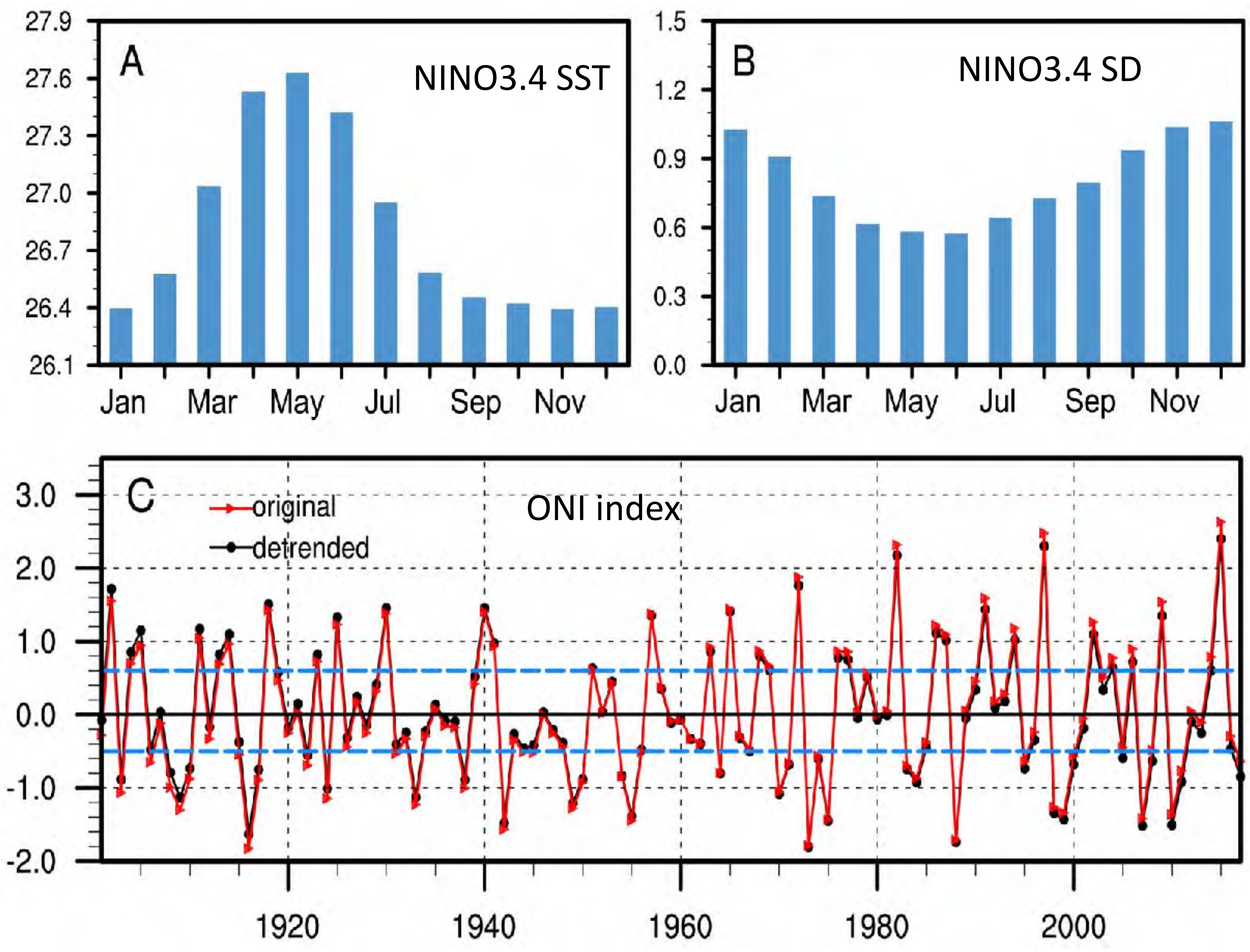

- Insignificant upward trend of 0.027k/decade (p=0.83). Black dotted line denotes the ONI after removing the linear trend.
- ONDJF ONI>0.6°C El Nino year. Total of 33 El Nino identified.
- Same El Niño years as those defined by NCEP/CPC except missing the marginal 1953 and 1979 El Niño events (1949-2017)

Object of analysis

Analysis focuses on the temporal evolution characteristics of the onset, development and mature of ENSO events, which is depicted by the equatorial SSTA (5˚S and 5˚N) and from the October of the year prior to El Niño occurrence to the October of the El Niño year (the Hovmöller diagram).

Nonlinear K-mean cluster analysis (Wilks 2011)

Squared Euclidean distance is used to measure the “similarity” between each cluster member and the corresponding cluster centroid.

Silhouette clustering evaluation criterion is used to evaluate the performance of cluster analysis.

Silhouette value, ranging from -1 to +1, for each member is a measure of the similarity between that member and other members in its own cluster, when compared to the members in other clusters.

A high silhouette value indicates that the member is well-matched to its own cluster, and poorly-matched to neighboring clusters (Kaufman & Rousseeuw, 2009).

We use K=4 clusters mainly based on physical consideration and its stability.

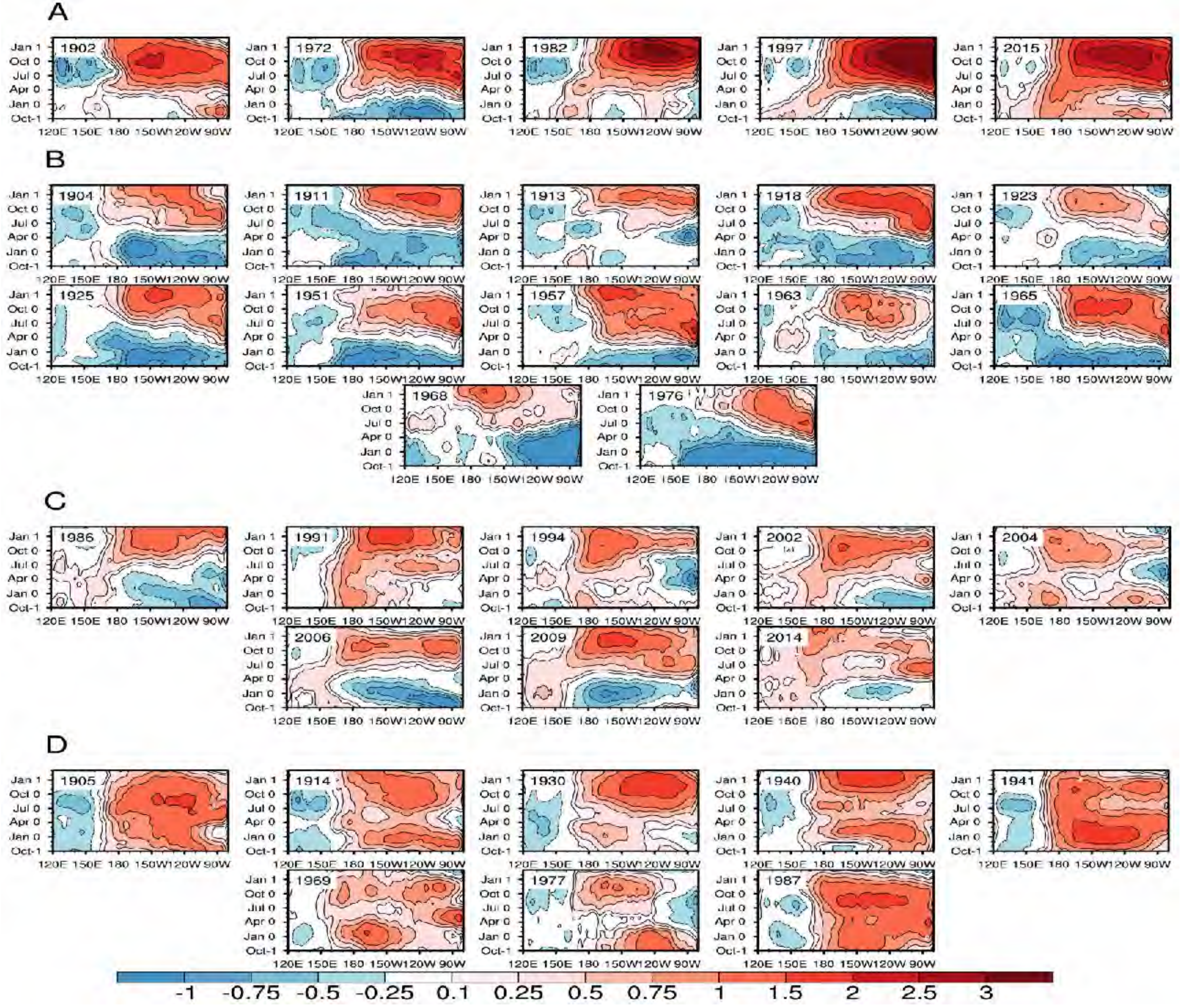

The equatorial SSTA evolution patterns for each individual El Niño event within each of the 4 clusters: (A) 5 strong BW, (B) 12 moderate EP, (C) 8 moderate CP, and (D) 8 Successive El Niño.

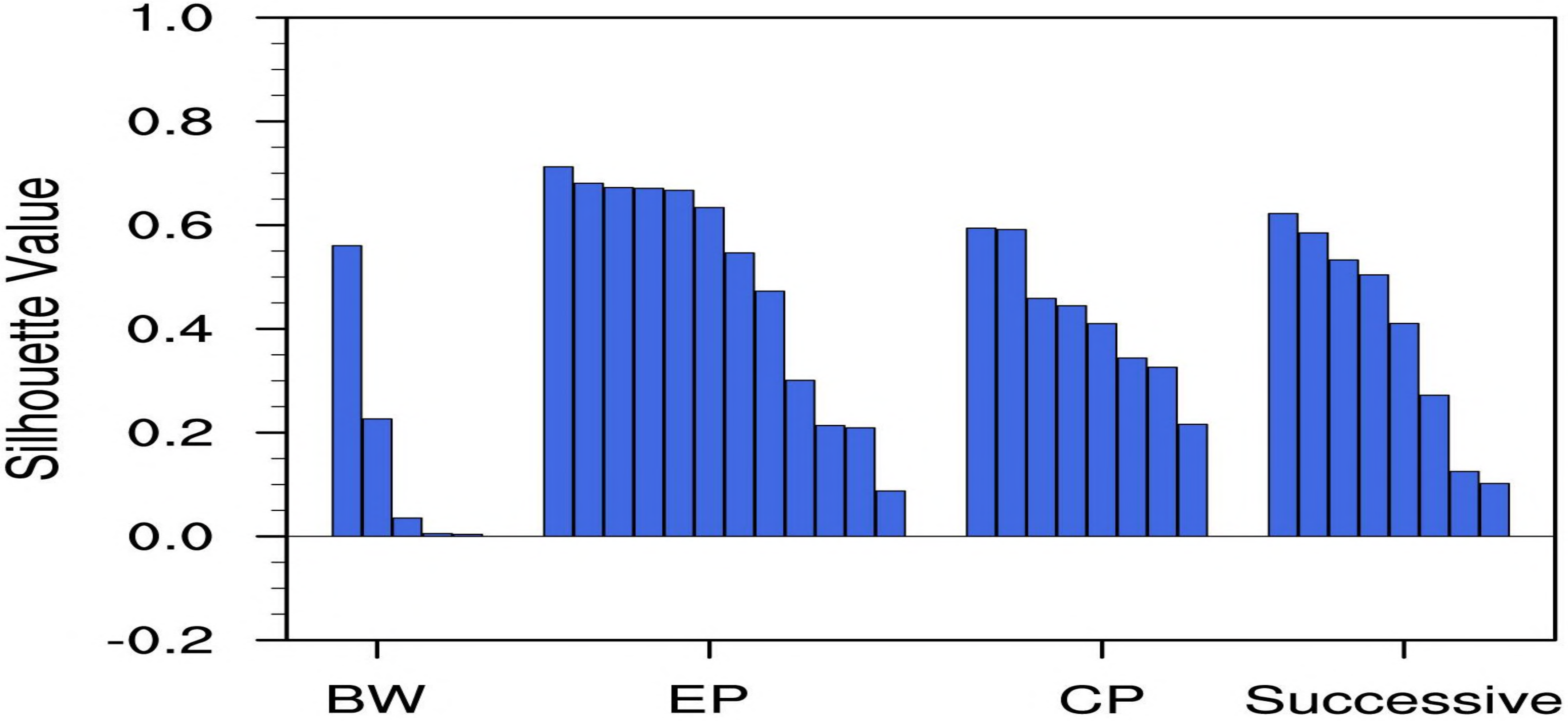

Silhouette values for each El Niño event within each of the 4 clusters for 1901-2017 period. The silhouette value, ranging from -1.0 to +1.0, is a measure of how similar a member is to other members in its own cluster when compared to the members in other clusters.

Composite SSTA evolution for 4 Clusters of El Nino development

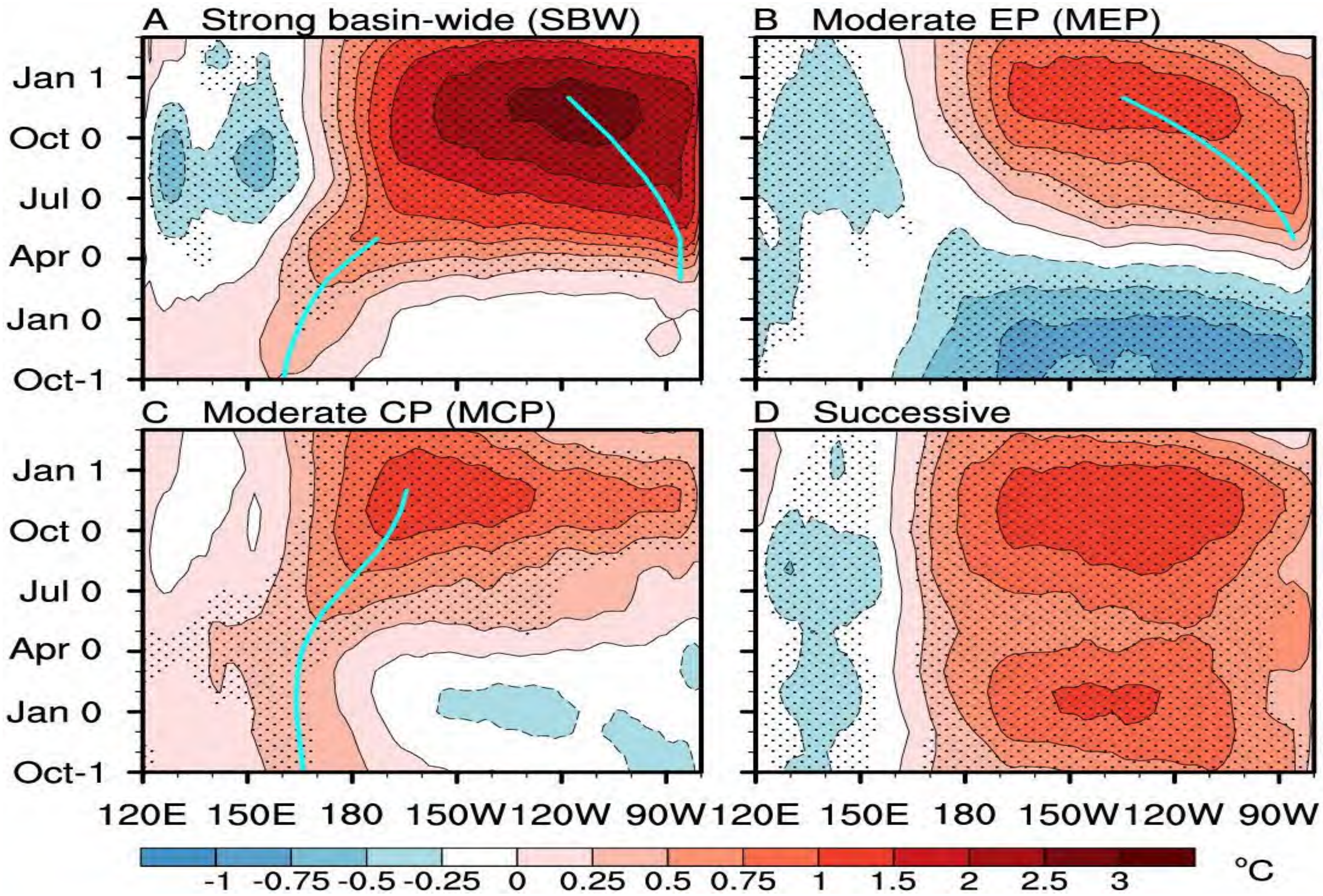

Composite longitude-time diagrams of the equatorial SSTA averaged between 5°S and 5°N.

The green lines outline the propagation tracks of maximum SSTAs.

Three types of dynamically distinguished El Niño events

Distinctive evolution features

Onset mechanisms:

involve distinctive dynamical processes.

Different Climate impacts

SST , surface zonal wind anomalies and maximum upward motion

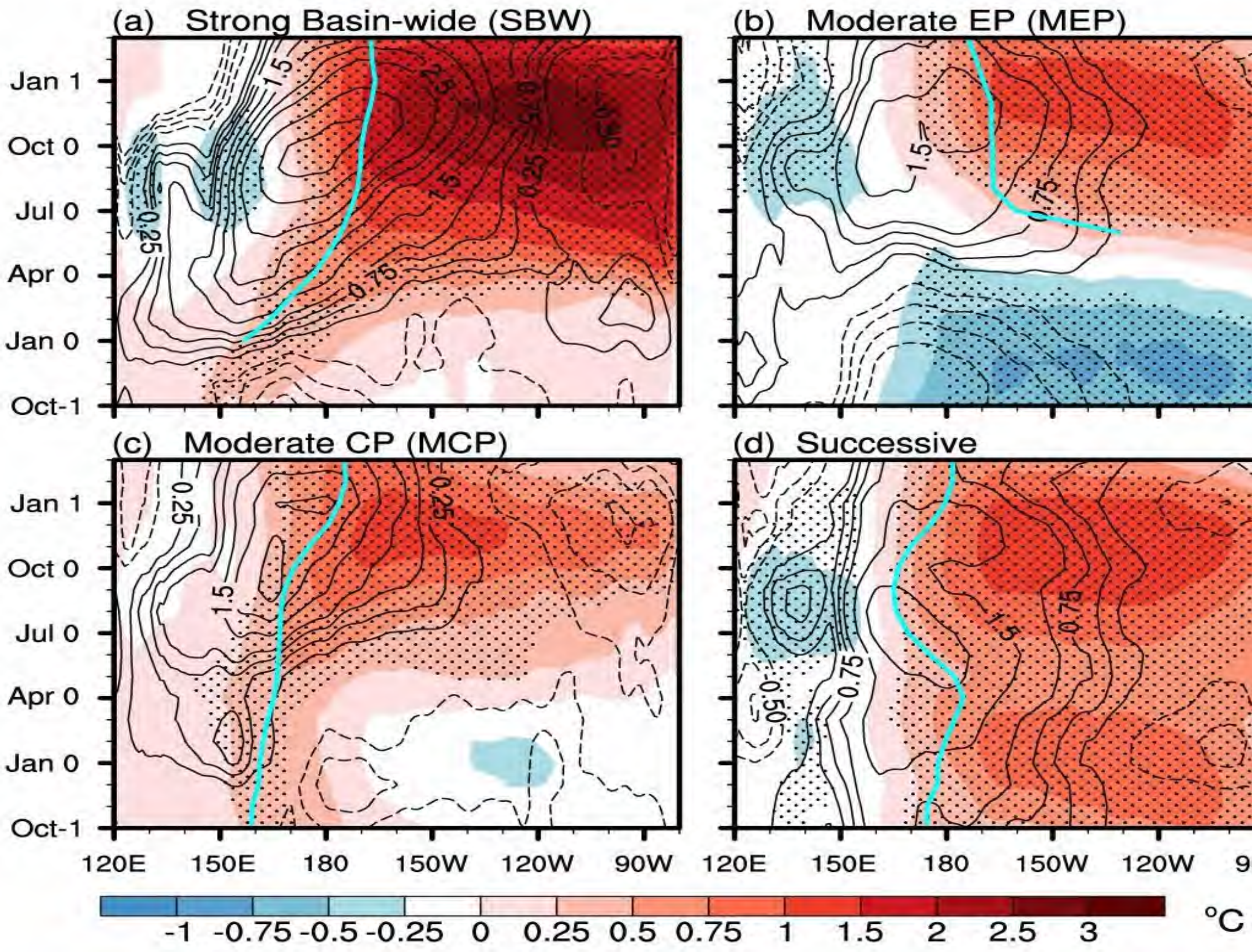

Evolution of the surface zonal wind and thermocline anomalies associated with three types of El Nino onset

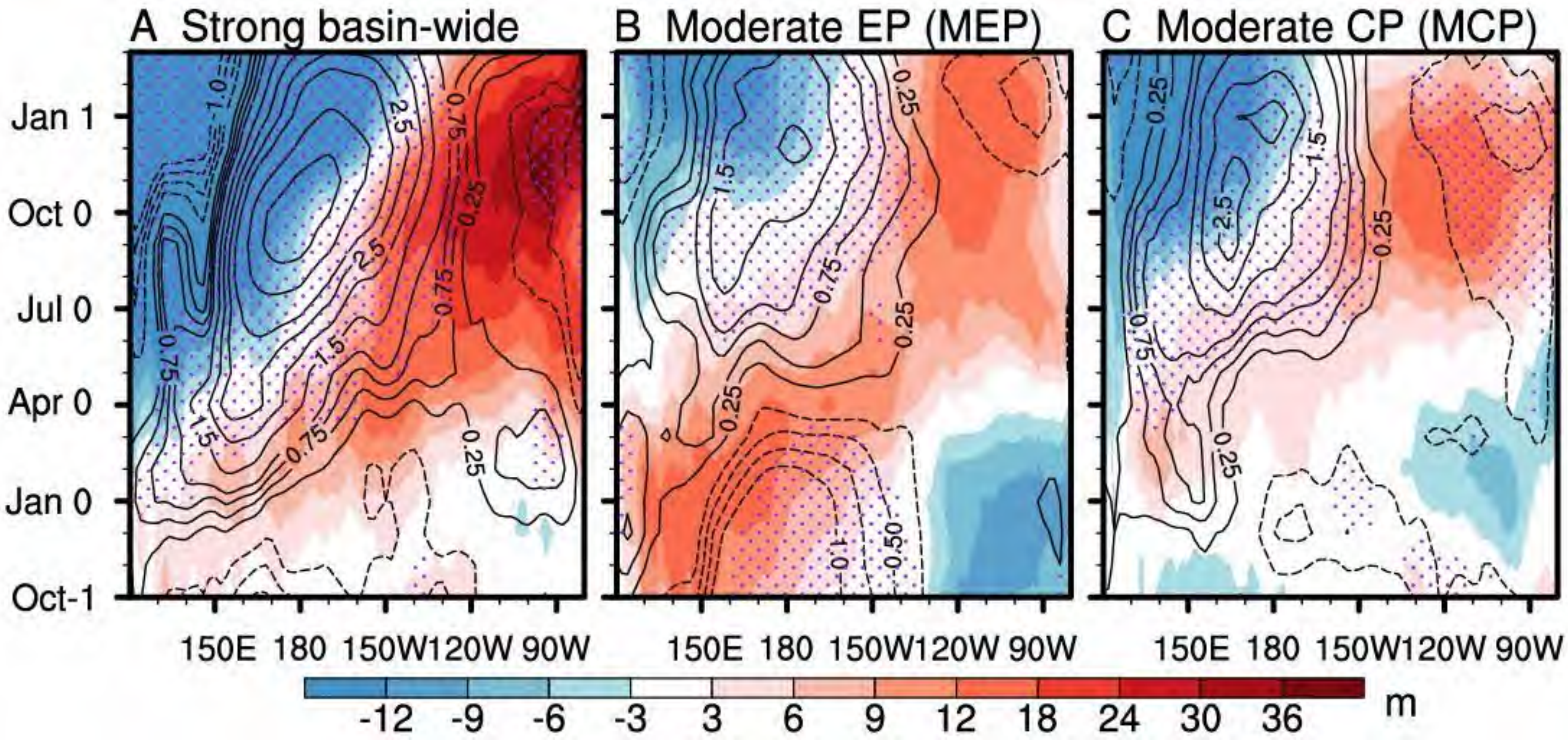

Comparison of equatorial zonal structure of the three types of El Nino

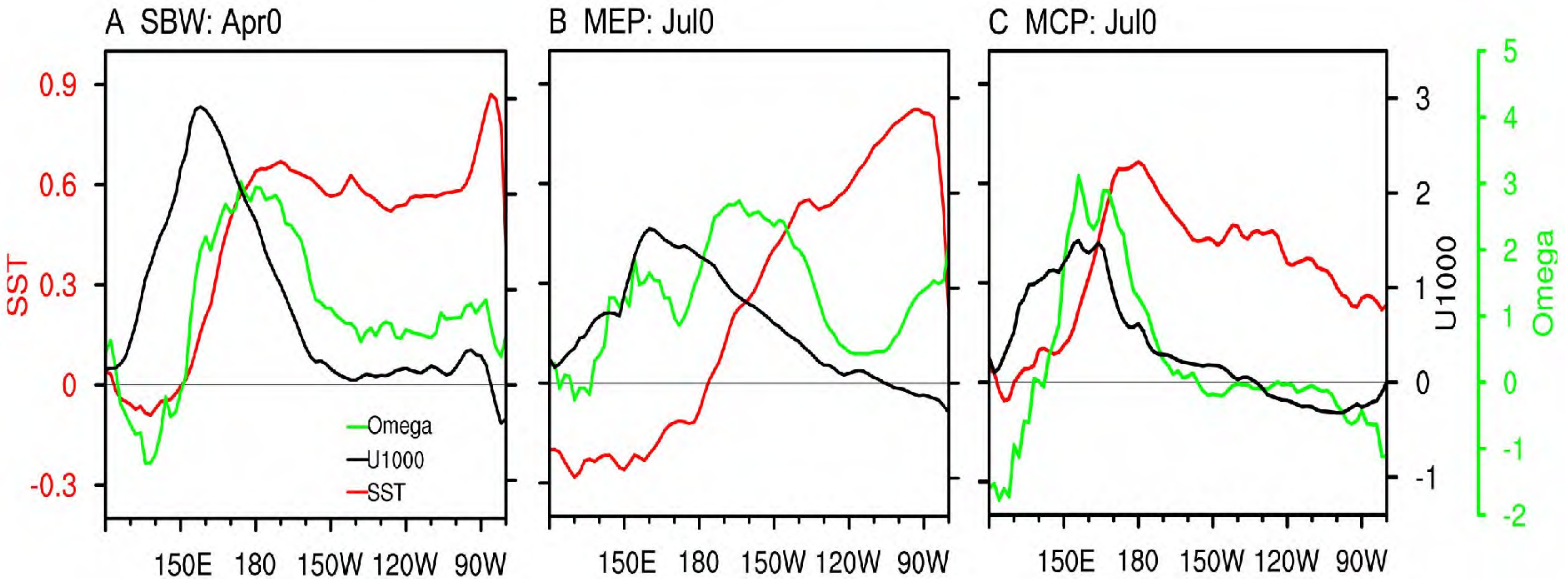

At onset time: (A) April(0) for Strong El Nino, (B) July(0) for MEP El Nino, and (C) July(0) for MCP El Nino. The figure shows the phase relationship among SSTA, zonal wind anomaly and convective anomaly.

Comparison of the characteristics of three types of onset

Phase	MCP	SBW	MEP
Pre-onset	Prolonged weak warming in WP	Initial warming and strong WWBs in WP	La Niña conditions
Onset	summer at CP	spring, basin-wide	summer at EP
Development processes	Zonal advective feedback	Zonal advective and thermocline/upwelling feedbacks	Thermocline feedback
SSTA propagation	eastward	eastward at onset	westward
Mature	~160°W (1.0-2.5K)	~120°W (>2.5K)	~140°W (1.0-2.5K)

Moderate central Pacific (MCP), strong basin-wide (SBW) and moderate eastern Pacific (MEP) events. WP means western Pacific.

Three types of dynamically distinguished El Niño events

Distinctive Onset features

Onsets involve distinctive dynamical processes.

Different Climate impacts

Ocean mixed layer heat budget

$$\frac{\partial T'}{\partial t} = -\left(\mathrm{V}' \cdot \nabla\overline{T} + \overline{\mathrm{V}} \cdot \nabla T' + \mathrm{V}' \cdot \nabla T'\right) + \frac{Q'_{net}}{\rho C_p H} + R$$

$$= -\left[\left(\frac{u'\partial\overline{T}}{\partial x} + \frac{\overline{u}\partial T'}{\partial x} + \frac{u'\partial T'}{\partial x}\right) + \left(\frac{v'\partial\overline{T}}{\partial y} + \frac{\overline{v}\partial T'}{\partial y} + \frac{v'\partial T'}{\partial y}\right) + \left(\frac{w'\partial\overline{T}}{\partial z} + \frac{\overline{w}\partial T'}{\partial z} + \frac{w'\partial T'}{\partial z}\right)\right] + \frac{Q'_{net}}{\rho C_p H} + R$$

Zonal advective feedback

upwelling feedback

Thermocline feedback

ρ(=10^3 kg m^{-3}) is water density;
C_p(=4000 J kg K^{-1}) is the specific heat of water;
H the mixed layer depth (50m)

Ocean mixed layer heat budget analysis of three types of El Niño

Region	ENSO Types	$-\frac{u'\partial\overline{T}}{\partial x}$	$-\frac{\overline{u}\partial T'}{\partial x}$	$-\frac{u'\partial T'}{\partial x}$	$-\frac{w'\partial\overline{T}}{\partial z}$	$-\frac{\overline{w}\partial T'}{\partial z}$	$-\frac{w'\partial T'}{\partial z}$
160°W-80°W	SBW	0.35	-0.06	-0.06	0.26	0.23	-0.11
	MEP	0.06	0.00	-0.01	-0.01	0.08	0.00
	MCP	0.15	-0.04	0.01	0.01	0.05	-0.01

during June-July-August of the El Niño developing year The units are: °C month^{-1}. The dominant feedback in each type of El Niño is marked red. The term $-\boldsymbol{u'\partial\overline{T}/\partial x}$, $-\boldsymbol{\overline{w}\partial T'/\partial z}$ and $-\boldsymbol{w'\partial\overline{T}/\partial z}$ represent the zonal advective feedback, thermocline feedback, and upwelling feedback, respectively.

Three types of dynamically distinguished El Niño events

Distinctive Onset features

Onset mechanisms:

involve distinctive dynamical processes.

Different Hydroclimate Impacts

Different rainfall anomalies associated with three types of El Nino onset

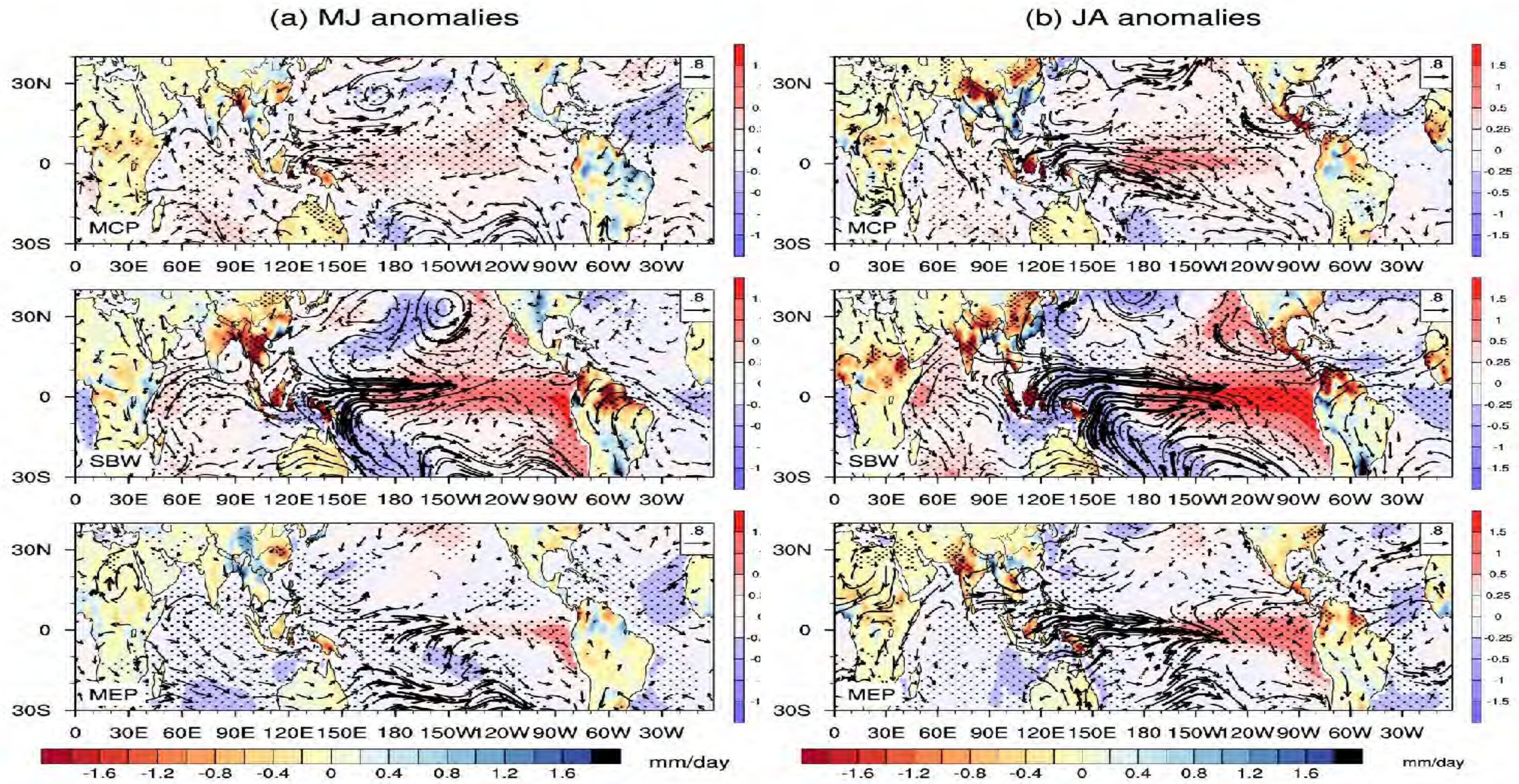

Comparison

1. the present categorization distinguishes strong and moderate El Niño events and also the first-year and successive El Niño.

2. The strong events originate from the WP (similar to the MCP) but mature in the EP (similar to the MEP) and they involve both the zonal advective feedbacks in the CP (as in the MCP-El Niño) and the thermocline feedback in the EP (as in the MEP-El Niño).

3. EP and CP classification mixed SBW and MEP because they are based on a snap shot of SSTA in the mature ohase.

4. SBW and MCP share common WP origin, but SBW events are distinguished from the MCP events by the prominent westerly anomalies in the western-CP occurring from January to April.

Change of the El Niño onset under the 20th century's climate change

How does El Nino types change ?
Why do they change?

Changing El Niño types from 1901 to 2017

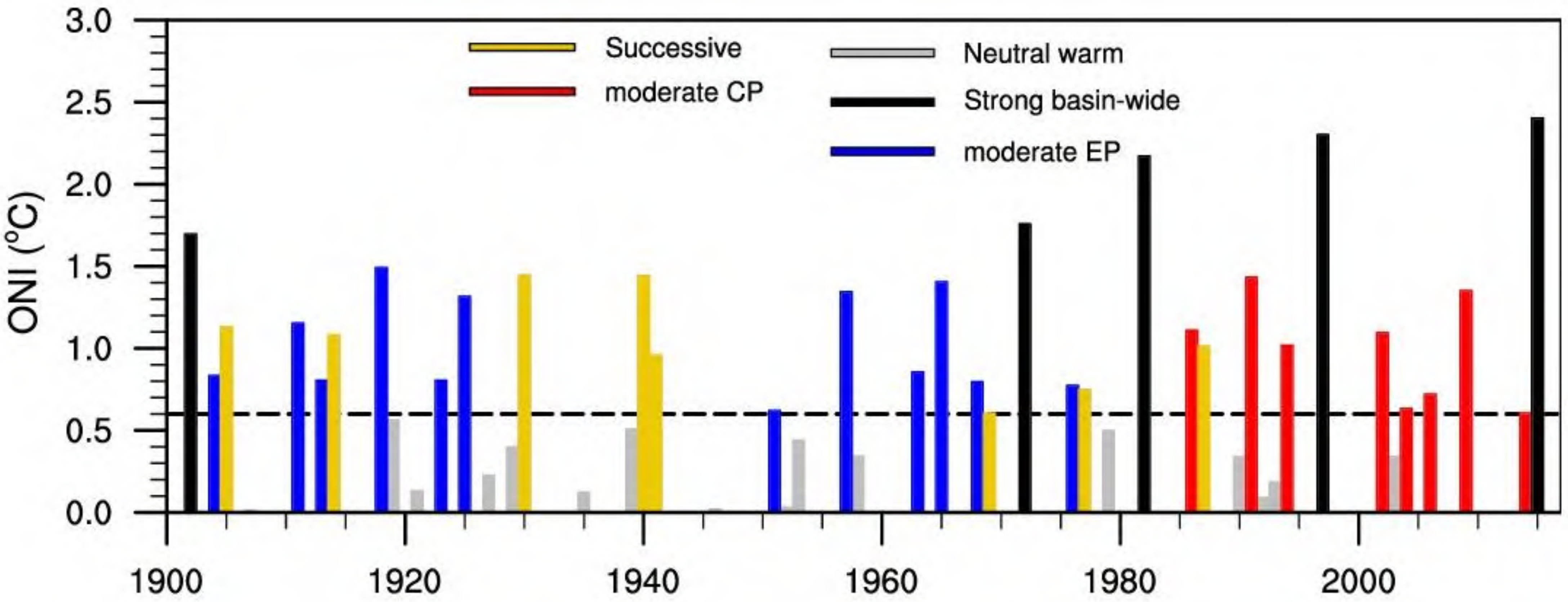

ONDJF ONI Bar diagram. The 33 El Niño events are shown in different color bars. Gray bars mark the remaining warm neutral years.

Contingent table testing significance of El Nino change

	MCP	SBW	MEP	Total
Pre-1978	0	2	12	12
Post-1978	8	3	0	13
Total	8	5	12	25

Contingent (two-way) table showing the regime change of El Niño between Pre-1978 and Post-1978. Shown are the numbers of the three types of El Niño events. The degree of freedom equals to 2 and Chi Square value equals to 20.1 ($p<0.001$).

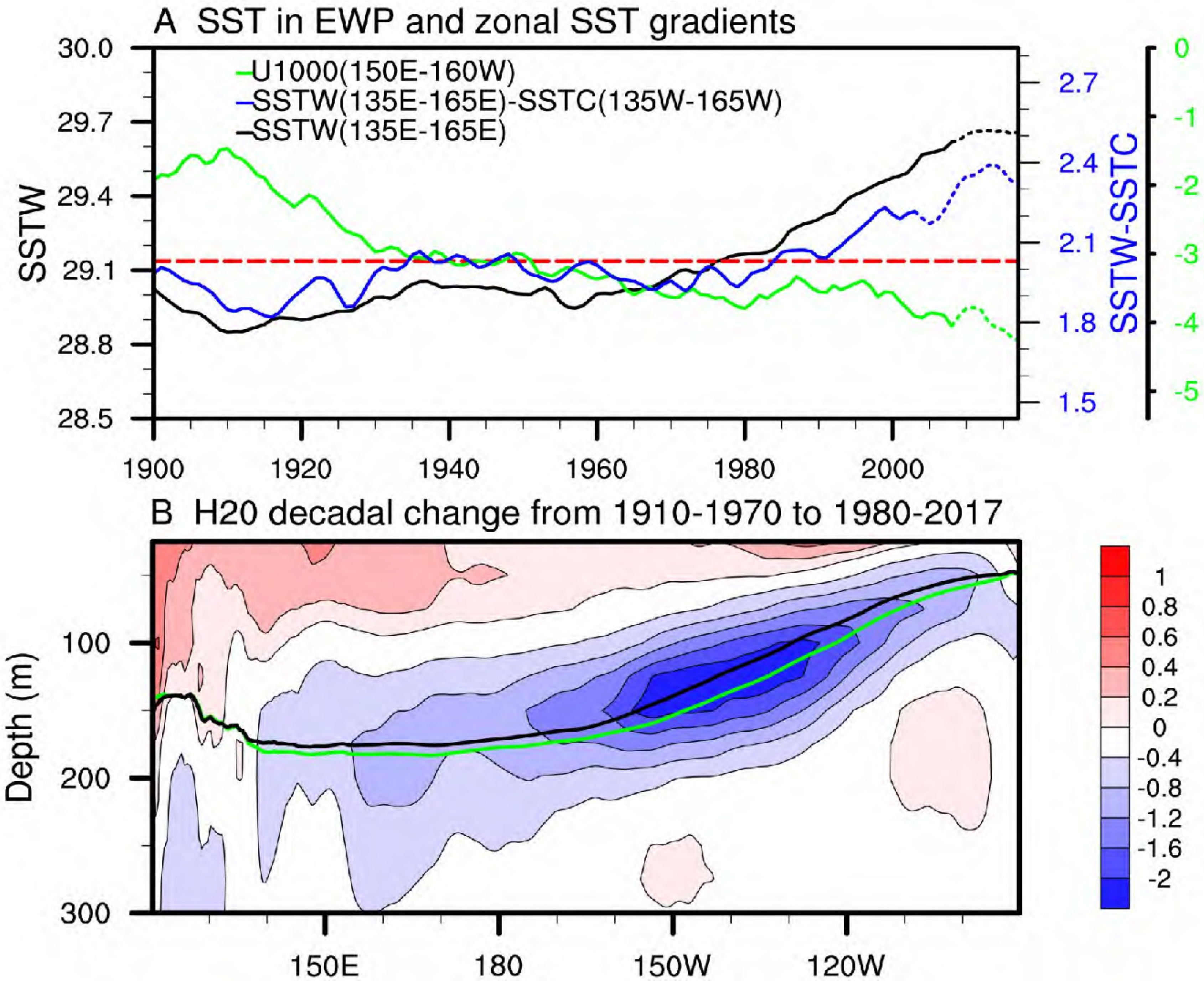

What has caused the observed change of El Niño regimes?

Change of the background state in the equatorial Pacific. The thermoclines in the MEP epoch (green) and CP (black) epoch are shown. The ocean stratification, defined as the difference between the mean temperature over the upper 75 m and the temperature at 100 m averaged over 150°E–140°W, increases from 0.9°C during MEP epoch to 1.5°C during the MCP epoch.

How the change of basic state could affect El Nino onset

These changes in the background conditions over the past four decades are arguably favorable for the occurrence of MCP and SBW El Niño events.

- The WP warming increases the zonal SST gradients across the dateline, thus enhances the zonal advective feedback process, which is conducive to El Niño being initiated in the NINO 4 (160°E-150°W) region.
- The WP warming provides favorable conditions for the Madden-Julian Oscillation (22) events to move into the western Pacific more frequently (23), increasing the frequency of WWBs and thereby the probability of occurrence of SBW events.
- The increased vertical temperature gradients strengthen the thermocline feedback, favoring occurrence of SBW events.

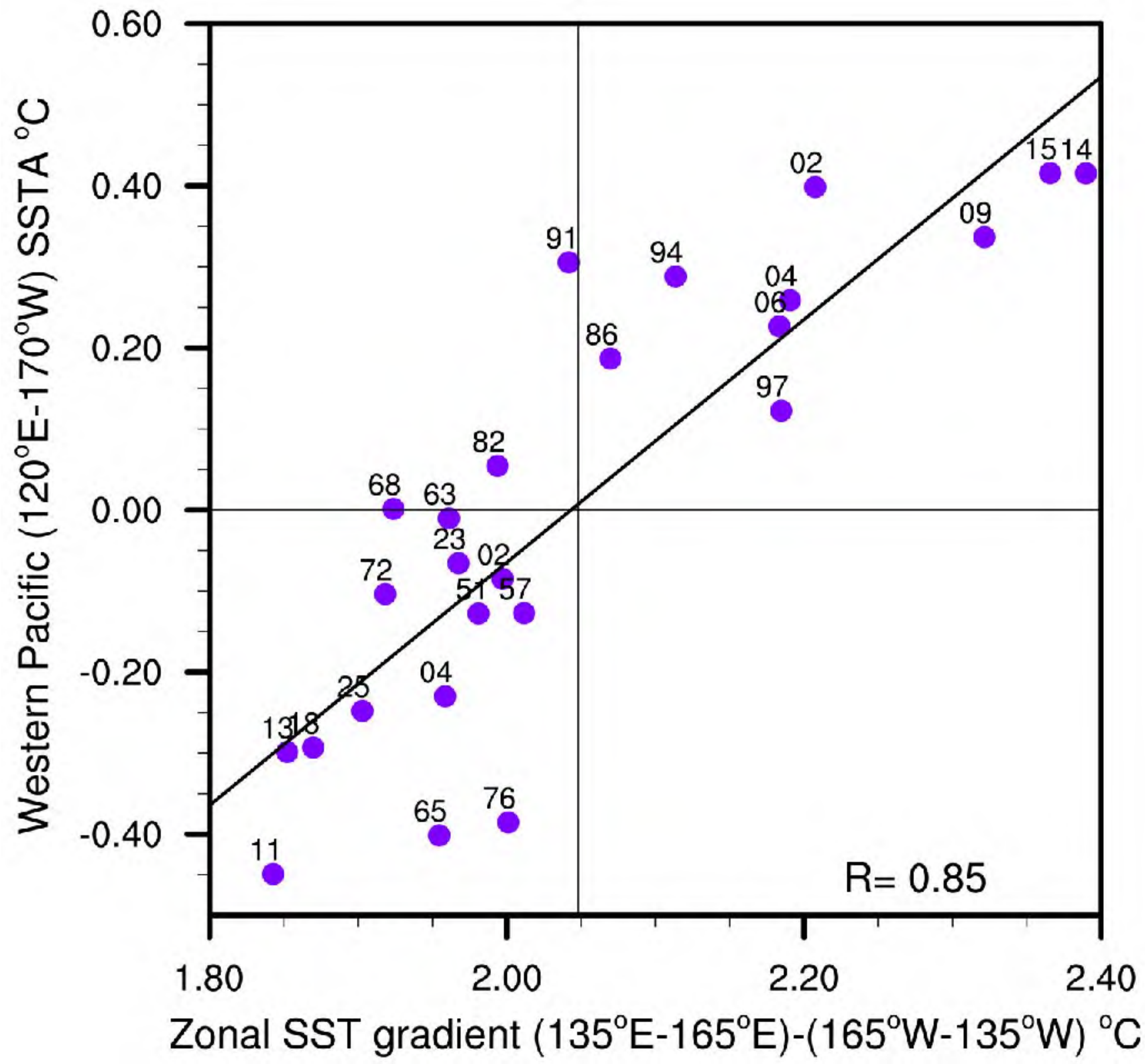

The NINO 4 warming is related to the increased background zonal SST gradient, which is conducive to El Niño being initiated in the WP

The mean state is defined by the 31-year running mean climatology. (25 first year onset events)

Implication for the future change of El Niño properties

The aforementioned observational analysis reveals the controlling factors that would lead to increased large-amplitude El Niño events in future.
We hypothesized that more frequent occurrences of SBW and MCP events require an enhanced zonal SST gradient in the central Pacific.

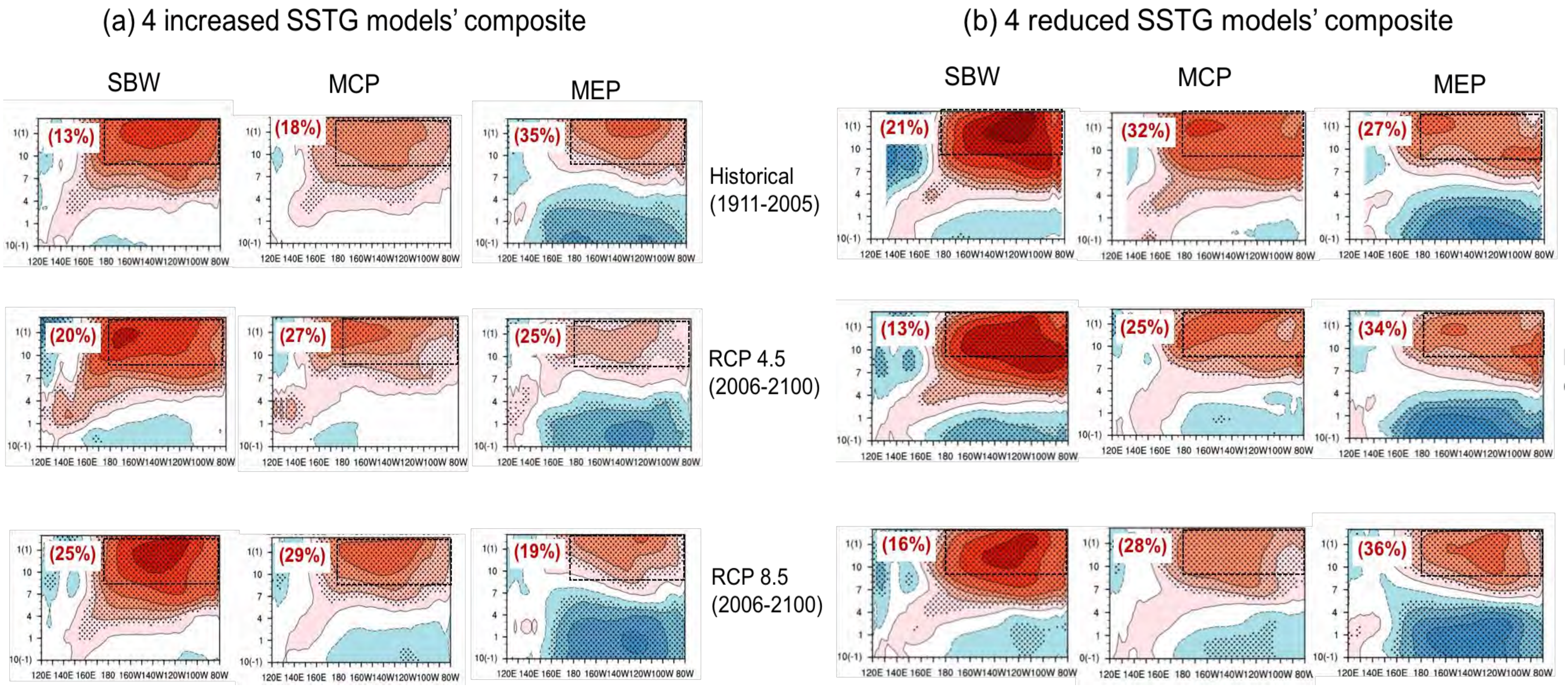

Composite evolutions of the equatorial Pacific SST anomalies in three types of El Niño onset, derived from CMIP5 coupled models. (A) composite evolution from 4 CMIP5 models that project an increased zonal mean SST gradient (SSTG) in the RCP 4.5 and RCP 8.5 scenario. (B) composite evolution from 4 models that project a decreased zonal mean SST gradient in the RCP 4.5 and RCP 8.5 scenario. To facilitate comparison, the period of integration is 95 yrs for both the historical run (1911-2005) and the RCP4.5 and RCP 8.5 run (2006-2100).

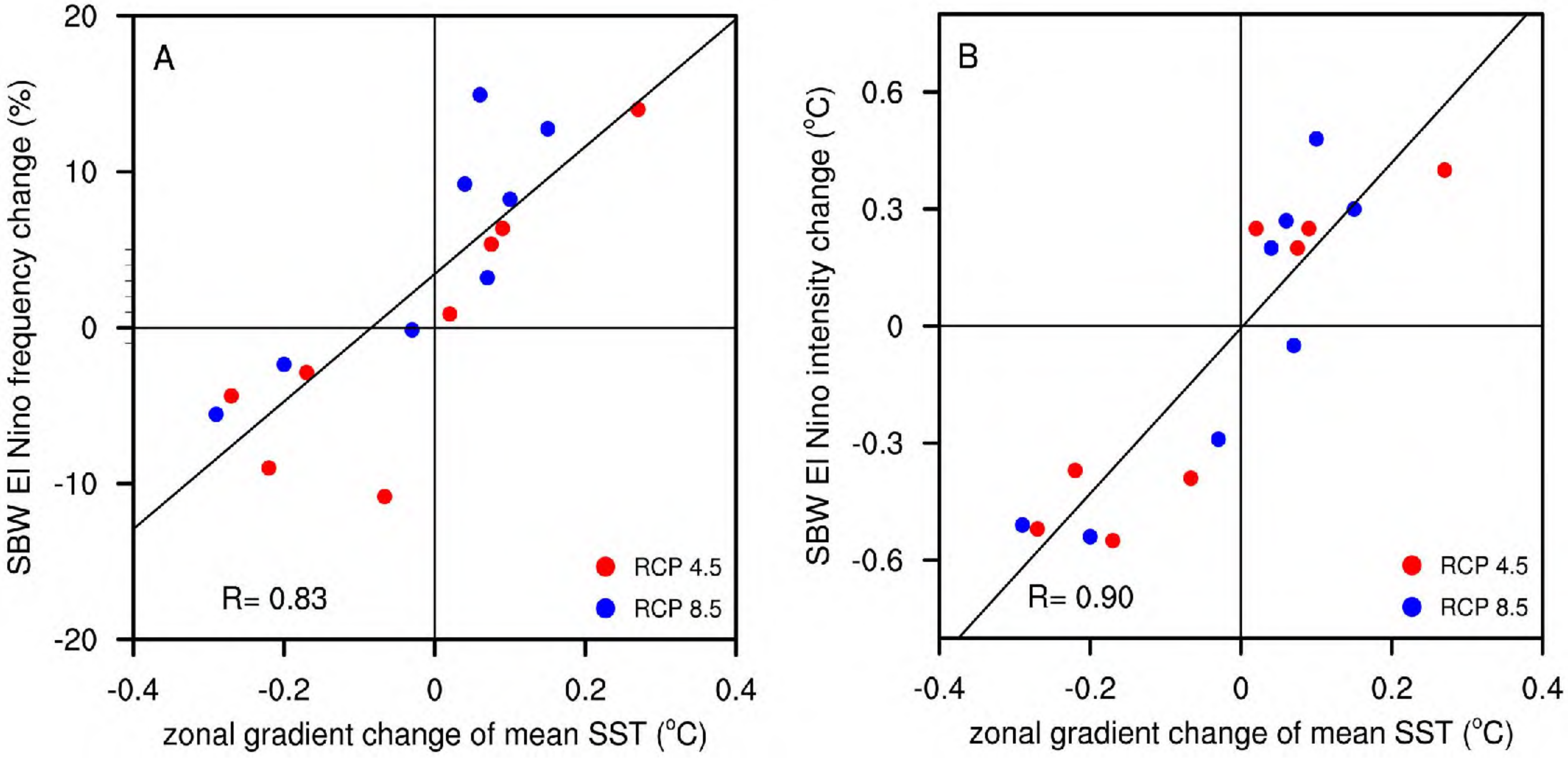

Dependence of the future change of strong basin-wide (SBW) El Niño events on the change of the mean-state zonal SST gradient measured by the WPSST (5°S-5°N, 150°-180°E) minus EPSST (5°S-5°N, 120°-150°W).

Major Findings

- Three types of El Niño onset are detected (SBW, MEP, MCP), which distinguish the strong from moderate events and exhibit distinct development mechanisms and global climate impacts.
- El Niño onset regime has changed from eastern Pacific-origin to western Pacific-origin with more frequent occurrence of extreme events since the 1970s.
- This regime change is hypothesized to arise from a background warming in the western Pacific and the associated increased zonal and vertical SST gradients in the equatorial central Pacific, which reveals a controlling factor that could lead to increased extreme El Niño events in future.
- Observation shows that increased zonal SST gradient in the central Pacific favors the development of warming in NINO 4 region.
- The CMIP5 models' projections demonstrate both the frequency and intensity of the strong El Niño events will increase significantly if the projected central Pacific zonal SST gradients enhance.
- The models' uncertainty in the projected equatorial zonal SST gradients, however, remains a major roadblock for faithful prediction of El Niño's future changes.

Discussions

- Root causes of the mean state change in 20th century
- Future change of extreme El Nino
- A Major road block for models' projection

Root cause of the mean state change in 20th century

The root causes of the observed background changes in the later part of the 20th century remain elusive.

Natural internal variability? Coupled GCMs can generate multidecadal variations of the mean state and ENSO diversity.

Change of El Niño in the late 1970s coincides with a rapid warming in the Indo-Pacific warm pool. But the recent global warming need not be due solely to anthropogenic forcing. Natural variability may have added significant contributions to the recent warming.

While we attribute the El Niño onset regime change to the mean SST gradient change, there is an alternative possibility that the mean state change is affected by the rectification effect of the randomly changing El Niño and La Niña due to their nonlinear asymmetry.

Future changes of the extreme El Nino

The future change of ENSO amplitude is an extremely important issue.

El Niño amplitude change is primarily determined by the frequency of SBW El Niño events; in addition, the SBW events tend to concur with MCP events.

More frequent occurrences of SBW and MCP events require enhanced SST gradients in the western-central Pacific which can enhance zonal advective feedback and increase the probability of WWB occurrence in the western Pacific.

In addition, increased upper-ocean vertical temperature gradients in the central-eastern Pacific may favor SBW events by enhancing the thermocline and upwelling feedbacks.

A Major road block for models' projection

The current generation of models has great difficulty in capturing the El Niño diversity and the projected Pacific mean state changes are highly uncertain due to models' biases in simulating mean states and ENSO.

The impact of climate change on the mean east-west gradient of SST in the tropical Pacific has been an issue of some debate. The "weak Walker circulation" theory versus ''ocean dynamical thermostat'' theory

The present work indicates that the uncertainty in the projected equatorial zonal SST gradients would prohibit faithful prediction of the El Niño's future change.

Application

The cluster analysis for delineating ENSO diversity provides a new metric for validation and improvement of climate models' capacity in reproducing the observed ENSO complexity, which is critical for improved ENSO prediction and reduced uncertainties in future projection of ENSO changes.

END

Additional figures

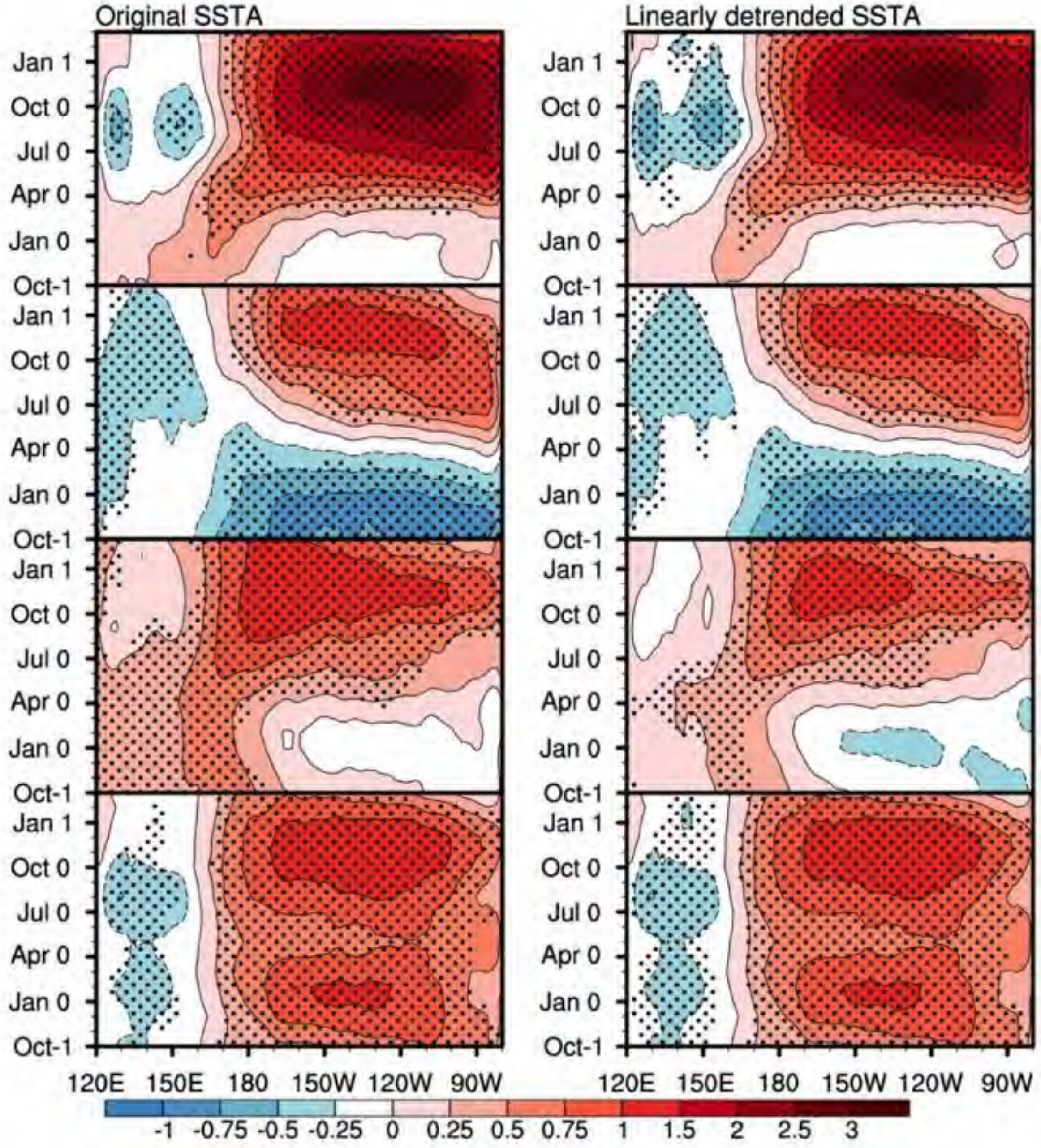

Figure S4 Composite maps of SSTA for each cluster derived from the original data (left panel) and the corresponding patterns from the detrended data (right panels) during 1901-2017 in units of °C.

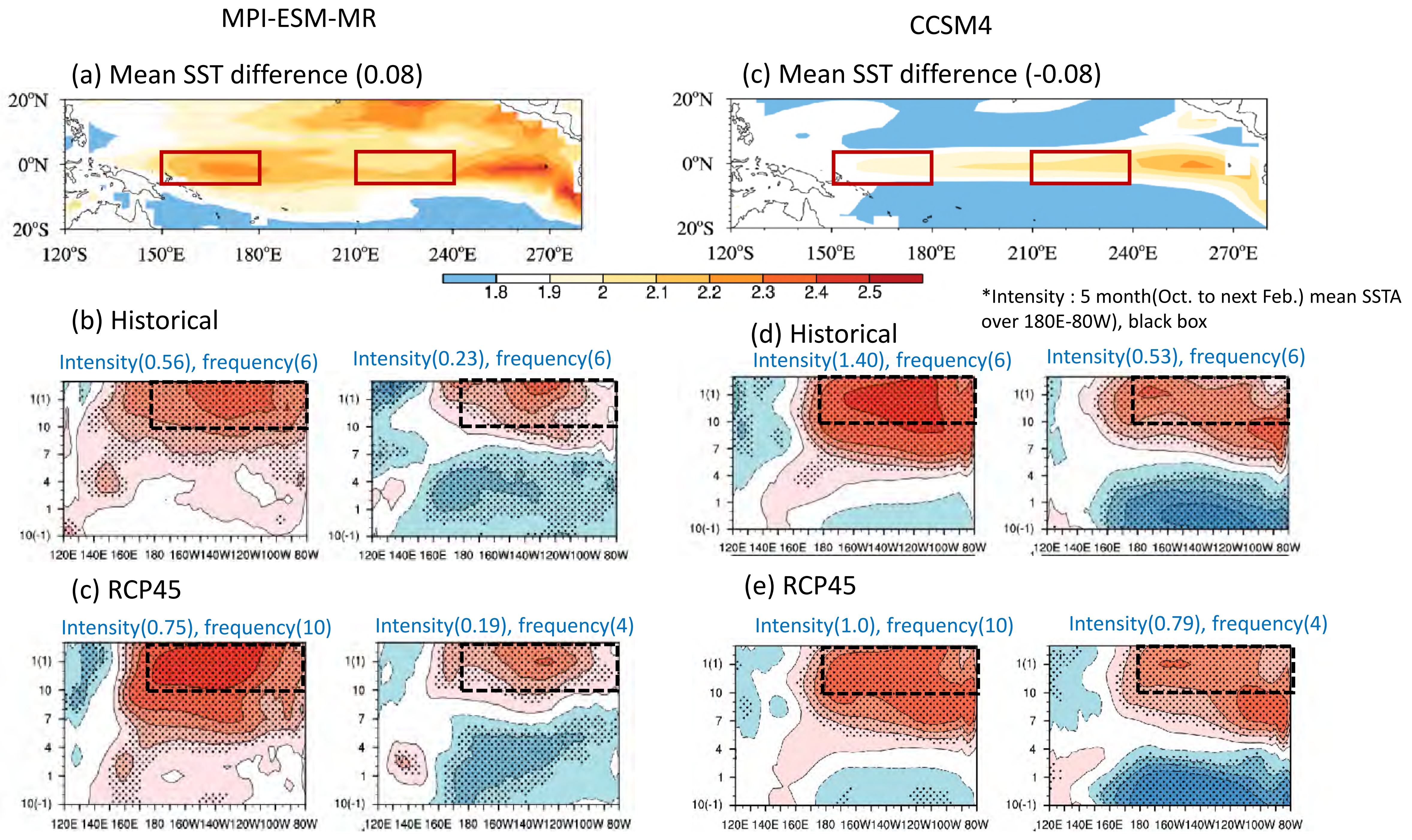

MPI-ESM-MR
CCSM4
(a) Mean SST difference (0.08)
(c) Mean SST difference (-0.08)
20°N
0°N
20°S
120°S
150°E
180°E
210°E
240°E
270°E
1.8
1.9
2
2.1
2.2
2.3
2.4
2.5
*Intensity : 5 month(Oct. to next Feb.) mean SSTA over 180E-80W), black box
(b) Historical
Intensity(0.56), frequency(6)
Intensity(0.23), frequency(6)
(d) Historical
Intensity(1.40), frequency(6)
Intensity(0.53), frequency(6)
(c) RCP45
Intensity(0.75), frequency(10)
Intensity(0.19), frequency(4)
(e) RCP45
Intensity(1.0), frequency(10)
Intensity(0.79), frequency(4)
1(1)
10
7
4
1
10(-1)
120E 140E 160E 180 160W140W120W100W 80W

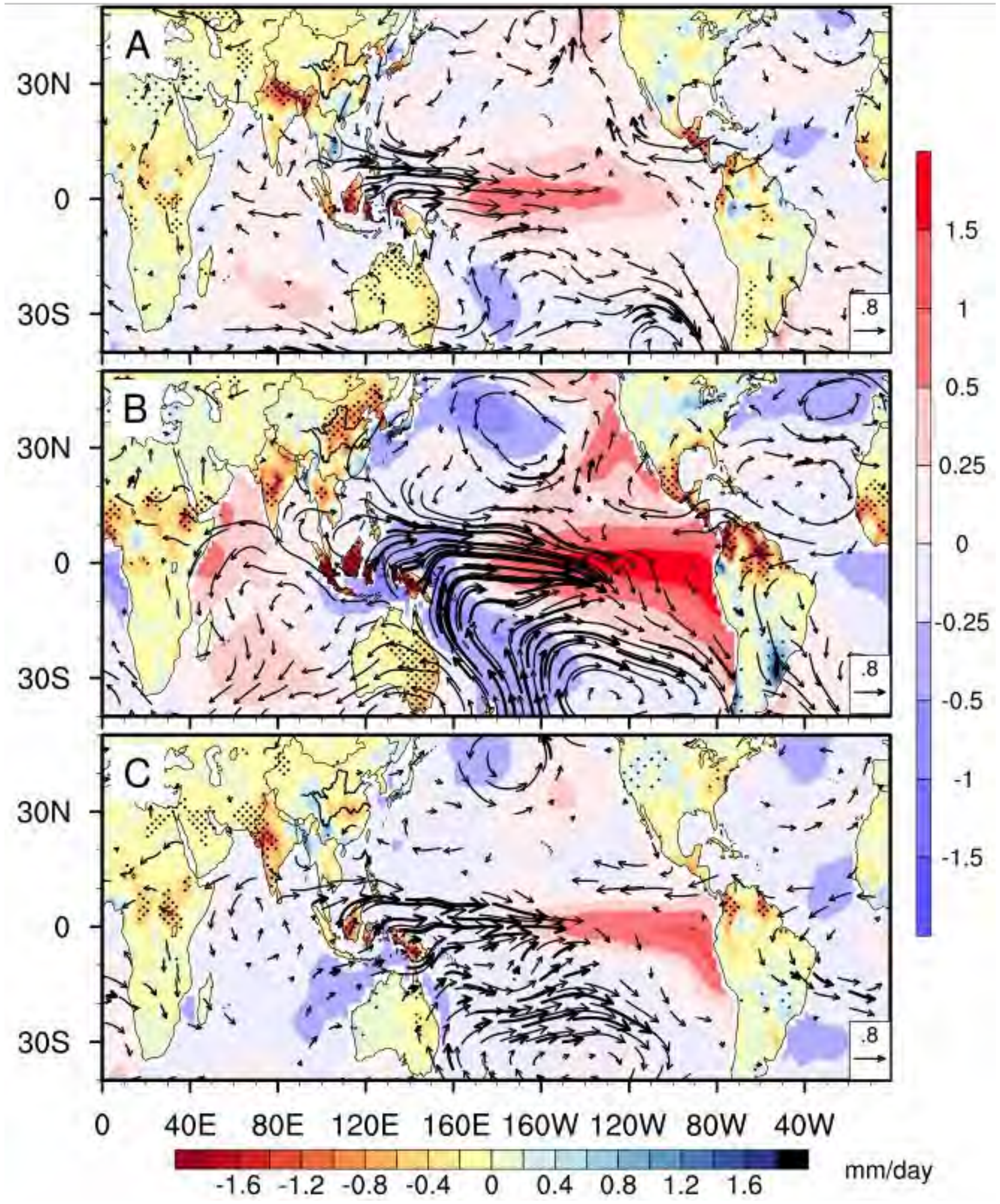

Figure S2 Different climate anomalies associated with three types of the first year El Niño during June-July-August-September: (A) moderate EP, (B) strong BW, and (C) moderate CP. The color shading over land represents composite precipitation anomalies. The color shading over ocean denotes composite SSTA in units of °C. The arrows denote composite 850hPa wind anomalies in units of m/s. The stippling denotes the regions where the signal (group mean) is larger than noise (the standard deviation of each member from the group mean). The thick arrows denote the composite wind anomalies that are significant at 95% confidence level. The data used are from 1901 to 2017. The data sources are described in Methods.

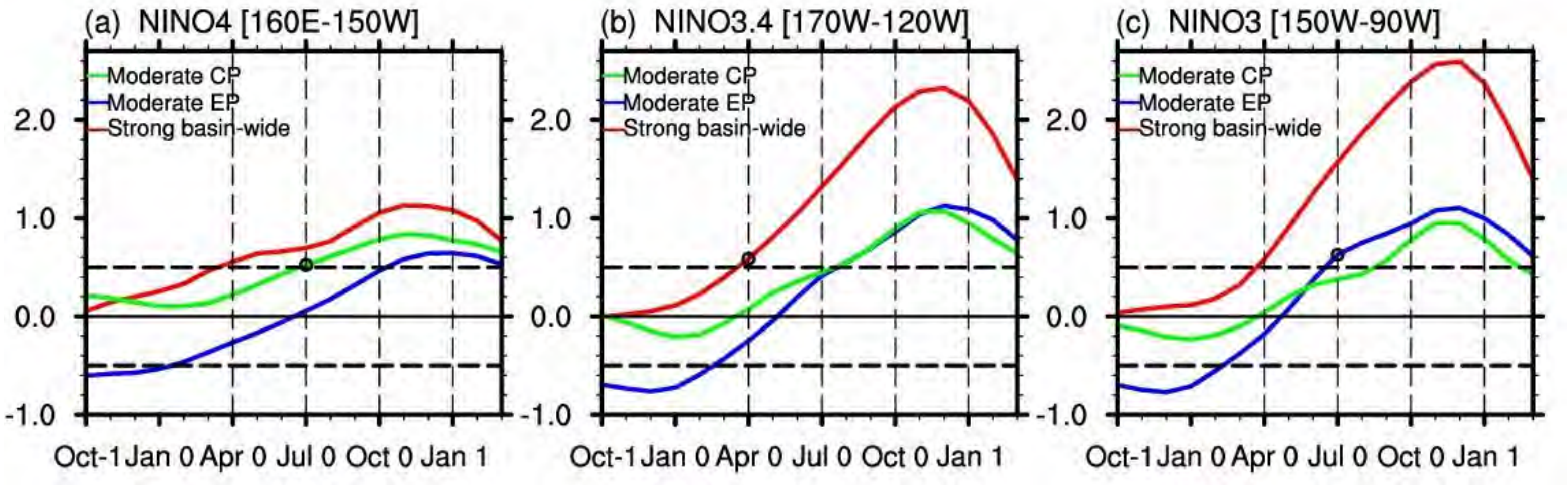

Extended Data Fig. 4 Comparison of evolutions of the three types of El Niño onset from pre-onset to mature phases as seen from (a) NINO 4, (b) NINO 3.4, and (c) NINO 3 regions, respectively. Shown are composite equatorial SSTA evolution from Oct (-1) to Mar (1) in units of °C. For convenience of comparison, the onset date is defined by the area averaged SSTA exceeding 0.5°C in any of the three NINO regions and each of them is marked by the empty circle. On average, the moderate CP events onset I July 0 in the NINO 4 region, the moderate EP events onset in July 0 in the NINO3 region, and strong BW events onset in April 0 nearly simultaneously in all three regions.